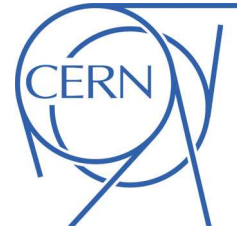


ATLAS NOTE

March 21, 2011



1 Search for Heavy Vector-like Quarks Coupling to Light Generations

2 First Author^a, Second Author^a, Third Author^b3 ^a*One Institution*4 ^b*Another Institution*

5 Abstract

6 We search for singly-produced quarks above the top mass in events with a W or Z bo-
7 son produced in association with two or more high transverse momentum jets. The vector
8 boson is reconstructed in the $W \rightarrow \ell\nu$ and $Z \rightarrow \ell\ell$ modes, where ℓ is an electron or a
9 muon. Using over 35 pb^{-1} of ATLAS 2010 data collected at a center-of-mass energy of 7
10 TeV, we fit the invariant mass of the system composed of the vector boson and the highest
11 transverse momentum jet to set limits on the heavy quark production cross section in terms
12 of a dimensionless parameter $\tilde{\kappa} = 1$. We find [insert limits].

13 Contents

14	1 Introduction	2
15	2 Monte Carlo datasets	2
16	2.1 Signals	2
17	2.2 Backgrounds	2
18	3 Data	2
19	4 Analysis	3
20	4.1 Object Definitions	3
21	4.1.1 Electron Selection	3
22	4.1.2 Muon Selection	3
23	4.1.3 Jet Selection	4
24	4.1.4 MET Cleaning	4
25	4.2 Pileup Reweighting	7
26	5 Systematic Uncertainties	7
27	5.1 $Q \rightarrow W + j$	10
28	5.1.1 QCD	10
29	5.1.2 Event selection	10
30	5.2 $Q \rightarrow Z + j$	11
31	5.2.1 Event Selection	11
32	6 Fit and Limit Calculation	12
33	6.1 Likelihood function	12
34	6.2 Limit calculation	12
35	6.3 Significance estimation	13
36	7 Results	13
37	8 Conclusion	13

1 Introduction

This is the introduction...

[1]

2 Monte Carlo datasets

2.1 Signals

Signals were generated with MadGraph, using the model $\nu l q$ obtained from the authors of the Tevatron paper [2]. For the purpose of this analysis, a U quark was used for the neutral current process and a D quark for the charged current, since these give the higher cross sections. The coupling to light quark u or d was taken to be $\tilde{\kappa} = \frac{M}{v}\kappa = 1$ and the branching ratio 100%. No cuts were applied for lepton acceptance of jet p_T . The CTEQ6L1 parton distribution function was used, with renormalization and factorization scales fixed at the Z (W) mass for the NC and CC signals respectively.

Official datasets for the neutral current and charged current processes of vector-like quark production were produced for the following mass points: 225, 300, 400, 500, 600, 700, 800, 900, and 1000 GeV. Each dataset consists of 20000 events where electron and muon channels are mixed. Tables 1 and 2 give the cross sections times Branching ratios for the neutral current process $pp \rightarrow Uq \rightarrow Zuq \rightarrow \ell^+ \ell^- uq$ and for the charged current process $pp \rightarrow Dq \rightarrow W^- uq \rightarrow \ell^- uq$ respectively, including processes with antiquarks. Validation plots can be found in:

<http://www.lps.umontreal.ca/twiki/bin/view/AtlasMontreal/NCValidationPlots>

<http://www.lps.umontreal.ca/twiki/bin/view/AtlasMontreal/TheValidationPlots>

Mass	cross section x BR (pb)	dataset number
225	5.91	115520
300	2.35	115521
400	0.849	115522
500	0.367	115526
600	0.178	115527
700	0.0938	115528
800	0.0525	115529
900	0.0307	115530
1000	0.0186	115531

Table 1: Cross section times branching ratio of neutral current events $pp \rightarrow U + jet$; $U \rightarrow Zu \rightarrow \ell^+ \ell^- u$ and $pp \rightarrow \bar{U} + jet$; $\bar{U} \rightarrow Z\bar{u} \rightarrow \ell^+ \ell^- \bar{u}$ with coupling $\tilde{\kappa} = 1$ and 100% BR($U \rightarrow Zu$)

2.2 Backgrounds

3 Data

This analysis uses pp collision data taken by the LHC in 2010, operating at a centre-of-mass energy of $\sqrt{s} = 7$ TeV. Application of basic detector and data-quality requirements results in an integrated luminosity of 36 pb^{-1} .

(missing luminosity uncertainty information, trigger information, etc)

Mass	cross section x BR (pb)	dataset number
225	41.80	115511
300	15.76	115512
400	5.47	115513
500	2.28	115514
600	1.07	115515
700	0.551	115516
800	0.299	115517
900	0.170	115518
1000	0.101	115519

Table 2: Cross section times branching ratio of charged current events $pp \rightarrow D + \text{jet}$; $D \rightarrow W^- u \rightarrow \ell^- \bar{\nu} u$ and $pp \rightarrow \bar{D} + \text{jet}$; $\bar{D} \rightarrow W^+ \bar{u} \rightarrow \ell^+ \nu \bar{u}$ with coupling $\tilde{\kappa} = 1$ and 100% BR($D \rightarrow Wu$)

63 4 Analysis

64 This is the intro to the analysis section

65 4.1 Object Definitions

66 In this section we describe the object definition and selection criteria for electrons, muons, jets, and
67 missing energy (E_T^{miss}) used in the analysis.

68 4.1.1 Electron Selection

69 Electron candidates are defined in much the same way as in the W+jets and Z+jets analyses [references].
70 They are required to be reconstructed by the Author 1 or 3 algorithms [reference]. They are required
71 to have $p_T > 20$ GeV and $|\eta| \leq 2.47$, excluding the crack region $1.37 < |\eta| < 1.52$. The p_T used
72 for a given electron is chosen dependent on whether there are a sufficient number of hits in the tracking
73 chamber. They are required to pass the 'medium' track and shape criteria of Ref. []. We also apply a
74 cleaning algorithm that vetos electrons reconstructed with faulty detector regions [OTX reference]. No
75 energy isolation requirement is applied for electrons. These criteria, as compared to the W+jets and
76 Z+jets analyses are summarized in Tab. 4.

77 4.1.2 Muon Selection

78 The muon definition and selection criteria are very similar to those used for the W+jets and Z+jets
79 analyses [refs]. Muons are reconstructed using combined track segments from different layers of the
80 muon chambers (mu_staco). Muon candidates are required to be reconstructed with an Author of 1 or 6.
81 We require that muon candidates pass the Inner Detector (ID) track quality criteria of Ref. []. They are
82 required to have $p_T > 20$ GeV and $|\eta| < 2.4$. An additional quality cut requires the fractional difference
83 between the transverse momenta deposited in the ID and Muon Spectrometer (MS) to be less than 0.5.
84 The separation between a muon and its nearest primary vertex is required to satisfy $z_0 < 10$ mm and
85 $d_0 < 0.1$ mm to reduce fakes by cosmic rays. A relative energy isolation requirement is made such that
86 $mu_{staco} p_{tcone20} / mu_{staco} p_t < 0.1$. Lastly, good muons are required to pass all of the muon quality
87 criteria defined by the Muon Combined Performance (MCP) group as specified in [reference]. These
88 selection criteria, and their differences with Z+jets and W+jets are summarized in Tab. 5.

89 4.1.3 Jet Selection

90 The jet selection criteria is very similar to the requirements imposed by the W/Z Standard Model groups
91 [<https://twiki.cern.ch/twiki/bin/view/AtlasProtected/SMWZjetsZxsec35pb>] and [<https://twiki.cern.ch/twiki/bin/view/AtlasPro>]
92 Here we give a brief description of those requirements used in this analysis.

93 Jets are reconstructed using the Anti-kt algorithm with a distance parameter of $R=0.4$. Standard
94 alignment correction and calibration procedures are applied according to [?]. Fully corrected jets are
95 required to have transverse momentum above 20 GeV and be within a pseudorapidity of $|\eta| \leq 4.5$. Jets
96 are removed if the Jet Vertex Fraction is $|JVF| \leq 0.75$ to help remove jets due to pile-up. Jets are removed
97 that fail a given set of ATLAS quality requirements [?] that protect against jets associated with in-time
98 energy depositions and noise effects in detectors used to reconstruct jets. Jets are removed if $\Delta R \leq 0.2$
99 between any lepton used to reconstruct a W or Z. These requirements are summarized in Table ??

100 4.1.4 MET Cleaning

101 To ensure that the quality of the missing transverse energy (E_T^{miss}) measurement, a MET cleaning is
102 performed. Events are rejected if there exists a jet with $p_T \geq 20$ GeV that is determined to be *BadMedium*
103 or *BadUngly* according to [?].

Process	cross section x BR x k-factor (pb)	generating efficiency	dataset tag
single top	7.152	1	108340.st_tchan_enu_McAtNlo_Jimmy
	7.176	1	108341.st_tchan_munu_McAtNlo_Jimmy
	7.128	1	108342.st_tchan_taunu_McAtNlo_Jimmy
	0.466	1	108343.st_schan_enu_McAtNlo_Jimmy
	0.468	1	108344.st_schan_munu_McAtNlo_Jimmy
	0.470	1	108345.st_schan_taunu_McAtNlo_Jimmy
	14.58	1	108346.st_Wt_McAtNlo_Jimmy
WZ	11.2	1	105940.McAtNlo_JIMMY_WpZ_lnuqq
	6.08	1	105970.McAtNlo_JIMMY_WmZ_lnuqq
WW	29.6	0.389	105985.WW_Herwig
$t\bar{t}$	144.1	0.556	105200.T1_McAtNlo_Jimmy
$Z \rightarrow \tau\tau$	802.0	1	107670.AlpgenJimmyZtautauNp0_pt20
	162.2	1	107671.AlpgenJimmyZtautauNp1_pt20
	49.29	1	107672.AlpgenJimmyZtautauNp2_pt20
	13.42	1	107673.AlpgenJimmyZtautauNp3_pt20
	3.538	1	107674.AlpgenJimmyZtautauNp4_pt20
	0.854	1	107675.AlpgenJimmyZtautauNp5_pt20
$Z \rightarrow \mu\mu$	802.4	1	107660.AlpgenJimmyZmumuNp0_pt20
	162.0	1	107661.AlpgenJimmyZmumuNp1_pt20
	48.31	1	107662.AlpgenJimmyZmumuNp2_pt20
	13.54	1	107663.AlpgenJimmyZmumuNp3_pt20
	3.416	1	107664.AlpgenJimmyZmumuNp4_pt20
	0.976	1	107665.AlpgenJimmyZmumuNp5_pt20
$Z \rightarrow ee$	807.5	1	107650.AlpgenJimmyZeeNp0_pt20
	162.6	1	107651.AlpgenJimmyZeeNp1_pt20
	49.17	1	107652.AlpgenJimmyZeeNp2_pt20
	13.66	1	107653.AlpgenJimmyZeeNp3_pt20
	3.294	1	107654.AlpgenJimmyZeeNp4_pt20
	0.976	1	107655.AlpgenJimmyZeeNp5_pt20
$W \rightarrow \tau\nu$	8340	1	107700.AlpgenJimmyWtaunuNp0_pt20
	1558	1	107701.AlpgenJimmyWtaunuNp1_pt20
	459.5	1	107702.AlpgenJimmyWtaunuNp2_pt20
	123	1	107703.AlpgenJimmyWtaunuNp3_pt20
	31.4	1	107704.AlpgenJimmyWtaunuNp4_pt20
	8.5	1	107705.AlpgenJimmyWtaunuNp5_pt20
$W \rightarrow \mu\nu$	8461	1	107690.AlpgenJimmyWmumuNp0_pt20
	1563	1	107691.AlpgenJimmyWmumuNp1_pt20
	457.9	1	107692.AlpgenJimmyWmumuNp2_pt20
	123.3	1	107693.AlpgenJimmyWmumuNp3_pt20
	31.4	1	107694.AlpgenJimmyWmumuNp4_pt20
	8.5	1	107695.AlpgenJimmyWmumuNp5_pt20
$W \rightarrow e\nu$	8434	1	107680.AlpgenJimmyWenuNp0_pt20
	1578	1	107681.AlpgenJimmyWenuNp1_pt20
	460.1	1	107682.AlpgenJimmyWenuNp2_pt20
	123.1	1	107683.AlpgenJimmyWenuNp3_pt20
	30.9	1	107684.AlpgenJimmyWenuNp4_pt20
	8.4	1	107685.AlpgenJimmyWenuNp5_pt20

Table 3: Cross section times branching ratio (times k-factor when applied), and generating efficiency for background datasets

Selection Criteria	W+jets	Z+jets	Heavy Quark
Author	1 or 3	1 or 3	1 or 3
p_T (GeV)	20 (ETCluster)	20 (track dependent)	20 (track dependent)
$ \eta $	2.47 (remove crack)	2.47 (remove crack)	2.47 (remove crack)
Reconstruction Quality	RobusterMedium	MediumWithTrackMatch	MediumWithTrackMatch
<i>DetectorQuality</i>	OTX Cleaning	OTX Cleaning	OTX Cleaning
Isolation	EtCone20pt ; 4GeV	-	-

Table 4: Electron selection criteria comparison to W+jets and Z+jets working groups.

Selection Criteria	W+jets	Z+jets	Heavy Quark
Collection	mu_staco_combined	mu_staco_combined	mu_staco_combined
Author	-	6	1 or 6
p_T (GeV)	$p_{TMS} > 10$ GeV	20	20
$ \eta $	2.4	2.4	2.4
p_T ID vs. MS	≥ 0.5	≥ 0.5	≥ 0.5
Cosmic Ray Veto	OTX Cleaning	OTX Cleaning	OTX Cleaning
Isolation	iso_cone_0.2/pt ; 0.1	iso_cone_0.2/pt ; 0.1	ptcone20/pt ; 0.1
MCP Quality	v15 [reference]	v16	v16

Table 5: List of muon selection criteria and comparison to W+jets and Z+jets analyses.

Selection Criteria	W+jets	Z+jets	Heavy Quark
Jet Collection	antikt4h1topo	antikt4h1topo	akt4topoem
Calibration	EMJES	EtaOffsetJES	EtaOffsetJES
p_T (GeV)	20	30	20
$ \eta $	2.8	4.5	4.5
$ JVF $	0.75	0.75	0.75
Veto Quality Criteria	v15 BadJets, UglyJets	v16 MediumBad	v16 MediumBad, MediumUgly

Table 6: Jet selection criteria comparison to W+jets and Z+jets working groups.

104 4.2 Pileup Reweighting

105 The Monte Carlo samples used were created with superimposed minimum bias events to simulate bunch
 106 train pileup. However, the amount of pileup in comparison to that in actual data was not modelled
 107 correctly. This can be seen by comparison of the distribution of the number of primary vertices (N_{PV}) in
 108 data and a Monte Carlo Sample in Figure[1]. To account for this discrepancy, reweighting factors were
 109 calculated in bins of N_{PV} to reweight Monte Carlo samples event by event to more accurately model the
 110 amount of pileup in data. These reweighting factors are calculated bin by bin as the fraction of events
 111 found in data to the fraction of events in Monte Carlo. These reweight factors are applied in all cutflows
 112 and histograms in both W and Z channels.

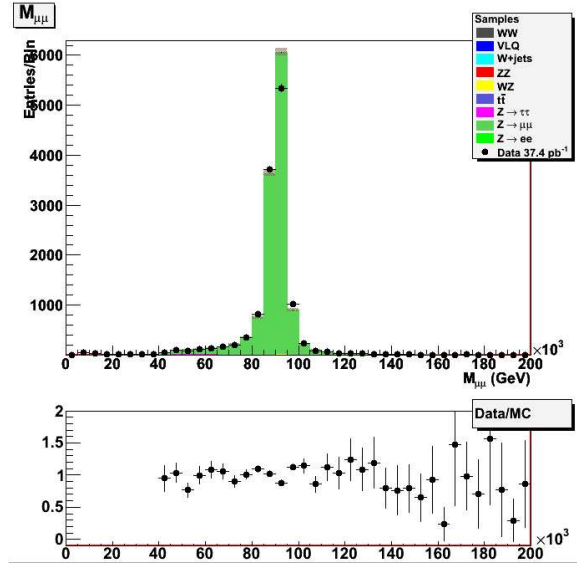


Figure 1: N_{PV} distributions normalized to unit area to compare the amount of pileup in data and Monte Carlo. The Monte Carlo sample shown is for $\rightarrow ee$ +jets but is indicative of all Monte Carlo samples due to the method in which pileup events are added.

113 5 Systematic Uncertainties

114 The main systematics considered here are due to Jet Energy Scale (JES), Jet Energy Resolution (JER),
 115 and Lepton Energy Scale (LES). The JES uncertainty was evaluated by comparing the values of accep-
 116 tance in the signal region between the nominal selection value and that in which the energy and momenta
 117 of each jet is scaled up (+) or down (-) by a scale factor. This factor is determined by using the JE-
 118 SUncertaintyProvider and is a function of jet p_T and η [reference]. The JER uncertainty was evaluated
 119 by comparing the acceptance between the nominal acceptance and that obtained when all jet energies
 120 and momenta are smeared once using the uncertainty obtained from the JERUncertaintyProvider that is
 121 a function of jet p_T and η [reference]. The LES uncertainty is obtained in the same fashion as the JES
 122 uncertainty but the smearing factors are obtained using the EnergyScalingProvider [reference]. These
 123 procedures were performed in all channels ($W \rightarrow e\nu$, $W \rightarrow \mu\nu$, $Z \rightarrow ee$, and $Z \rightarrow \mu\mu$). Results are
 124 shown in Tables 7, 8, 9, and 10. The total systematic uncertainty is taken as the quadrature sum of the
 125 individual uncertainties.

Mass Point (GeV)	JES(up,down)	JER	LES	Total
225	0.002654/ - 0.002904	± 0.002053	± 0.0003	
300	0.002653/ - 0.003654	± 0.000951	± 0.0005	
400	0.002954/ - 0.003205	± 0.000150	± 0.0010	
500	0.002854/ - 0.003305	± 0.000851	± 0.0011	
600	0.003071/ - 0.003138	± 0.000200	± 0.0014	
700	0.003809/ - 0.002506	± 0.000301	± 0.0017	
800	0.002856/ - 0.003307	± 0.000451	± 0.0005	
900	0.002405/ - 0.003107	± 0.001754	± 0.0002	
1000	0.002456/ - 0.003759	± 0.003709	± 0.0009	

Table 7: $Z \rightarrow \mu\mu$ systematic uncertainties in fractional differences between nominal acceptance and acceptance with given uncertainty applied.

Mass Point (GeV)	JES(up,down)	JER	LES(up,down)	Total
225	0.002153/ - 0.002553	± 0.000150	0.000651/ - 0.001101	
300	0.002303/ - 0.002303	± 0.000751	0.000350/ - 0.001201	
400	0.001853/ - 0.002754	± 0.000851	0.000300/ - 0.001002	
500	0.001652/ - 0.003054	± 0.001402	0.000300/0.000000	
600	0.003205/ - 0.003004	± 0.001402	0.000067/ - 0.000401	
700	0.002807/ - 0.002907	± 0.000702	0.000702/0.000000	
800	0.003056/ - 0.002756	± 0.000050	0.000100/0.000000	
900	0.002756/ - 0.003407	± 0.001603	0.000150/ - 0.000351	
1000	0.002907/ - 0.003108	± 0.003158	0.000050/ - 0.000150	

Table 8: $Z \rightarrow ee$ systematic uncertainties in fractional differences between nominal acceptance and acceptance with given uncertainty applied.

Q_d mass [GeV]	jet energy scale	jet energy resolution	muon energy scale
225	+0.0237 - 0.0261	± 0.0169	± 0.0015
300	+0.0173 - 0.0188	± 0.0192	± 0.0010
400	+0.0121 - 0.0148	± 0.0148	± 0.0039
500	+0.0126 - 0.0179	± 0.0179	± 0.0027
600	+0.0110 - 0.0129	± 0.0148	± 0.0043
700	+0.0161 - 0.0225	± 0.0164	± 0.0062
800	+0.0157 - 0.0174	± 0.0149	± 0.0069
900	+0.0154 - 0.0194	± 0.0076	± 0.0065
1000	+0.0165 - 0.0175	± 0.0172	± 0.0066

Table 9: Systematic uncertainties in the $W \rightarrow \mu\nu$ channel signal region. Uncertainties are displayed as the fractional difference between nominal acceptance and acceptance with $\pm 1\sigma$ uncertainty.

Q_d mass [GeV]	jet energy scale	jet energy resolution
225	+0.0321 - 0.0369	± 0.0356
300	+0.0223 - 0.0200	± 0.0188
400	+0.0170 - 0.0215	± 0.0403
500	+0.0172 - 0.0212	± 0.0249
600	+0.0100 - 0.0206	± 0.0295
700	+0.0163 - 0.0166	± 0.0280
800	+0.0122 - 0.0148	± 0.0199
900	+0.0164 - 0.0167	± 0.0275
1000	+0.0168 - 0.0142	± 0.0368

Table 10: Systematic uncertainties in the $W \rightarrow e\nu$ channel signal region. Uncertainties are displayed as the fractional difference between nominal acceptance and acceptance with $\pm 1\sigma$ uncertainty. The electron energy scale uncertainty is not displayed here because its contribution to uncertainty is negligible.

126 **5.1** $Q \rightarrow W + j$

127 In this section, we describe the QCD and event selection for the $W \rightarrow e\nu$ and $W \rightarrow \mu\nu$ channels.

128 **5.1.1** QCD

129 While it is possible to diminish QCD backgrounds substantially by cutting on E_T^{miss} , it is difficult to re-
130 move it completely without cutting out a large fraction of signal events. In the W channel, we incorporate
131 QCD into the backgrounds in order to improve the power of our limit calculation. Our QCD template
132 comes from different sources for the electron ($W \rightarrow e\nu$) and muon ($W \rightarrow \mu\nu$) channels.

133 For the $W \rightarrow \mu\nu$ channel we get our QCD template from Monte Carlo using the following sample:

134 `MuonQCDSample`

135 The normalization comes from fitting the missing energy in RooFit after cutting out events with $E_T^{miss} <$
136 10 GeV. In the $W \rightarrow e\nu$ channel we were unable to find a Monte Carlo sample that provided sufficient
137 statistics. Instead, we use a data-driven method in which we apply identical cuts to those used for picking
138 non-QCD events, except for the following differences:

- 139 • The electron trigger is changed from `EF_e15_medium` to `EF_g20_loose`, which is designed to
140 select photons.
- 141 • We reverse the tracking requirement by selecting 'loose' photons rather than 'medium' electrons.
- 142 • An isolation cut is imposed...

143 To get the QCD normalization in the $W \rightarrow e\nu$ channel, we use the same fitting technique that is used in
144 the $W \rightarrow \mu\nu$ channel.

145 **5.1.2** Event selection

146 **5.2** $Q \rightarrow Z + j$

147 This section introduces the $Q^- \rightarrow Z + j$ analysis

148 **5.2.1 Event Selection**

149 6 Fit and Limit Calculation

150 We perform a binned maximum likelihood fit to the vector-like quark invariant mass to extract the number
 151 of measured signal events and the upper limit at 95% confidence. The fit is performed separately for
 152 each signal mass. In this section we describe the probability density functions, signal extraction, limit
 153 calculation, and significance estimation.

154 6.1 Likelihood function

155 The binned likelihood \mathcal{L} can be written as:

$$\mathcal{L} = \prod_i \frac{f_i^{n_i} e^{-f_i}}{n_i!}, \quad (1)$$

156 where the product is over i bins, f_i is the expected number of events in bin i according to the fit model,
 157 and n_i is the number of observed events in bin i . The histogram f_i is the sum of signal and background
 158 histograms, weighted by their number of events as determined in the fit:

$$f_i = N_{\text{sig}} f_i^{\text{sig}} + N_{\text{bkg}} f_i^{\text{bkg}}. \quad (2)$$

159 The signal and background histogram shapes are determined from the Monte Carlo simulations as de-
 160 scribed earlier, except for the QCD component of the evj final state.

161 To incorporate systematic uncertainties on the signal and background rates, the following modifica-
 162 tions are made...

163 All free parameters in the fit to data except for N_{sig} are collectively referred to as nuisance parameters,
 164 θ .

165 6.2 Limit calculation

166 We adopt the procedure recommended by the ATLAS statistics group [ref]. We define our test statistic
 167 $q(N_{\text{sig}})$ as follows:

$$q(N_{\text{sig}}) = \begin{cases} -2 \log \left(\mathcal{L}(N_{\text{sig}}, \hat{\theta}) / \mathcal{L}(\hat{N}_{\text{sig}}, \hat{\theta}) \right), & N_{\text{sig}} \geq \hat{N}_{\text{sig}} \\ 0, & N_{\text{sig}} < \hat{N}_{\text{sig}} \end{cases} \quad (3)$$

168 As in [ref] we adopt the convention that a single caret over a variable name indicates the best-fit value,
 169 while a double-caret indicates the best fit value given other constraints. So, $\hat{\theta}$ denotes the best-fit nuisance
 170 parameters for a given fixed value of N_{sig} . The observed test statistic in the data for a given N_{sig} is denoted
 171 $q(N_{\text{sig}}|\text{data})$.

172 In the ideal case, the probability distribution $g(q(N_{\text{sig}}))$ is a χ^2 with one degree of freedom, regardless
 173 of N_{sig} . (If necessary: However, we find that this is frequently not the case with our fit model – figures #,
 174 #. Therefore, we determine the distribution of $q(N_{\text{sig}})$ using psuedoexperiments based on the fit model.)

175 The upper limit on the number of observed signal events at 95% confidence, is determined by solving
 176 the following equation for N_{sig} .

$$0.05 = \int_{q(N_{\text{sig}}|\text{data})}^{\infty} g(q(N_{\text{sig}})) dq(N_{\text{sig}}) \quad (4)$$

177 Sanity checks, expected limit bands.

178 **6.3 Significance estimation**

179 **7 Results**

180 This section gives the results of the analysis including limit extraction

181 **8 Conclusion**

182 This section for the conclusions

183 **References**

184 [1] S. L. Glashow, *Partial Symmetries of Weak Interactions*, Nucl. Phys. **22** (1961) 579–588.

185 [2] A. Atre, M. Carena, T. Han, and J. Santiago, *Heavy Quarks Above the Top at the Tevatron*, Phys.
186 Rev. **D79** (2009) 054018, arXiv:0806.3966 [hep-ph].